Momentum distribution in the unitary Bose gas from first principles

Tommaso Comparin and Werner Krauth
Laboratoire de Physique Statistique, École Normale Supérieure/PSL Research University, UPMC, Université Paris Diderot, CNRS, 24 rue Lhomond, 75005 Paris, France
(Dated: November 3, 2016)

Supplementary Item (i): Momentum-distribution estimator

In path-integral quantum Monte Carlo, the momentum distribution is usually computed from the exponential $e^{-i\mathbf{k}\cdot(\mathbf{x}-\mathbf{y})}$ (with open ends $\mathbf{x}$ and $\mathbf{y}$), averaged over open-path configurations[1, 2]. At large momenta k – where $n(\mathbf{k})$ tends to zero – this estimator becomes unpractical, because of a vanishing signal-to-noise ratio. We construct a new estimator (used in Fig. 3(e)), based on the solution of the two-body problem represented in Fig. S1[3]. We analytically

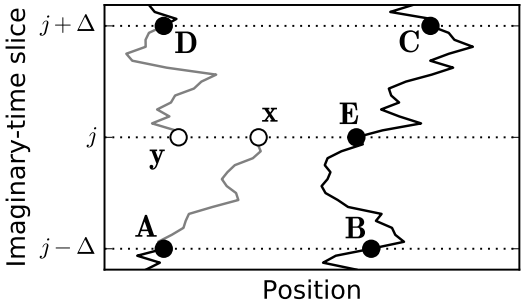

FIG. S1. Open $N = 2$ path configuration. An estimator for the momentum distribution is derived from the analytical expression for $n(\mathbf{k})$ for fixed positions $\mathbf{A}, \mathbf{B}, \mathbf{C}, \mathbf{D}, \mathbf{E}$.

determine $n(\mathbf{k}|\mathbf{A}, \ldots, \mathbf{E})$, the average of $e^{-i\mathbf{k}\cdot(\mathbf{x}-\mathbf{y})}$ for given positions $\mathbf{A}, \mathbf{B}, \mathbf{C}, \mathbf{D}, \mathbf{E}$. For $N = 2$, $n(\mathbf{k})$ is obtained as an average of $n(\mathbf{k}|\mathbf{A}, \ldots, \mathbf{E})$ over configurations $\mathbf{A}, \mathbf{B}, \mathbf{C}, \mathbf{D}, \mathbf{E}$ sampled during the simulation. For $N \geq 3$, this coarse-grained estimator holds for "local" configurations, where the two open ends are close to each other and to the nearest of the other bosons ($\mathbf{x} \sim \mathbf{y} \sim \mathbf{E}$). For non-local configurations we again resort to the direct estimator $\left\langle e^{-i\mathbf{k}\cdot(\mathbf{x}-\mathbf{y})} \right\rangle$, and finally obtain $n(\mathbf{k})$ as a weighted average of the two estimators (*cf.* Ref. [3]). This procedure relies on an appropriate cutoff between local and non-local configurations. At high enough temperature, where the procedure is used, we carefully check that the contact density c_2 extracted from the asymptotic behavior of $n(\mathbf{k})$ for $k \to \infty$ agrees with the $r \to 0$ limit of $g^{(2)}(\mathbf{r})$ (see Fig. 3(c)).

Supplementary Item (ii): Contact density at low temperature

In Fig. S2, the data of Fig. 3(a) are plotted as a function of T/T_c^0 , for a three-body cutoff $R_0\rho^{1/3} \simeq 0.184$. Our first-principles low-temperature values for $c_2\rho^{-4/3}$ are roughly compatible with the zero-temperature approximate results from Refs. [4–6]. These are obtained via a Jastrow ansatz and hypernetted-chain approximation[4], a quantum Monte Carlo calculations based on a Jastrow-Feenberg ansatz[5], and a time-dependent variational ansatz for the many-body state[6]. The value $c_2\rho^{-4/3} \simeq 22$, extracted from an analysis of the experimental data[7], appears significantly larger than our theoretical predictions.

Supplementary Item (iii): Superfluid transition

The critical temperature T_c is extracted from finite-N data using the scaling ansatz of Ref. [8]. This assumes that in the critical region the rescaled superfluid fraction $N^{1/3}\rho_s/\rho$ depends on the system size N only through the quantity $N^{1/(3\nu)}(T - T_c)/T_c$, where ν is the correlation-length critical exponent, and implies that $N^{1/3}\rho_s/\rho$ becomes

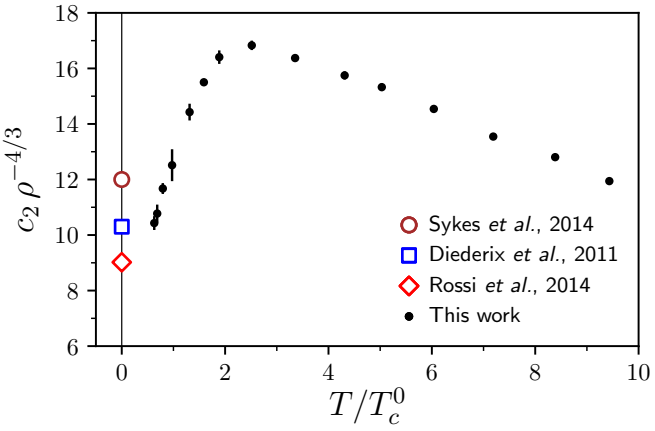

FIG. S2. Contact density at low temperature ($T/T_c^0 = 1$ corresponds to $\lambda_{\rm th}\rho^{1/3} = 1.377$), for $R_0\rho^{1/3} = 0.184$ (*black points*), and zero-temperature approximate results for the models in Refs. [4–6] (*open symbols*).

size-independent at the critical temperature $T = T_c$ of the infinite system. The dependence of $N^{1/3}\rho_s/\rho$ on system size, for different values of the three-body cutoff $R_0\rho^{1/3}$, is shown in Fig. S3, and we observe that the crossing point is roughly at 90% of the critical temperature of ideal bosons[9]. The critical temperature T_c weakly depends on $R_0\rho^{1/3}$: In the range $0.164 \lesssim R_0\rho^{1/3} \lesssim 0.204$, it increases from $T_c/T_c^0 \approx 0.87$ to $T_c/T_c^0 \approx 0.91$.

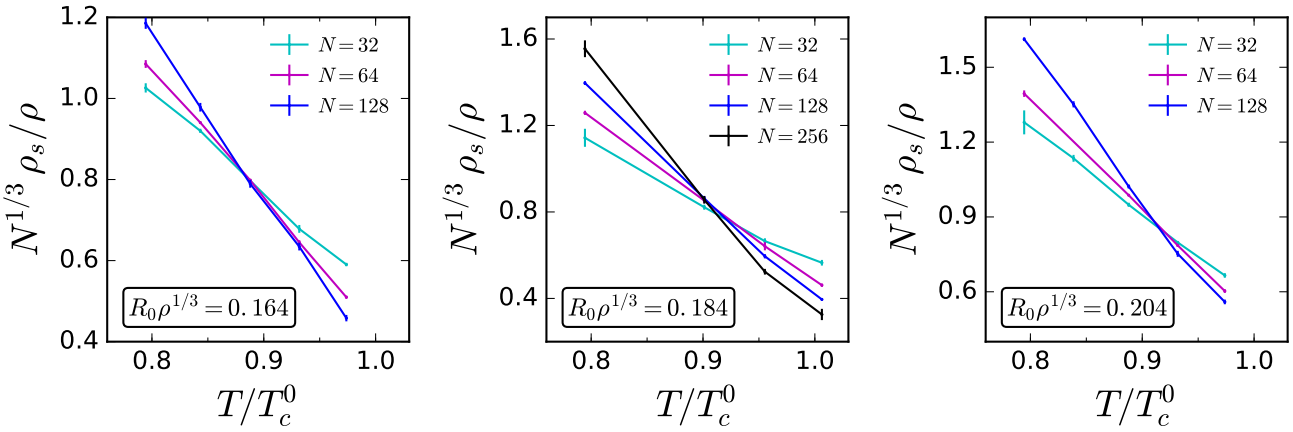

FIG. S3. Finite-size scaling of the superfluid fraction for different values of the three-body cutoff $R_0\rho^{1/3}$. The crossing point of $N^{1/3}\rho_s/\rho$ *vs.* T/T_c^0 establishes a 10% decrease of the superfluid transition temperature with respect to ideal bosons, in the limit $N \to \infty$ (*cf.* Fig. 4(c)).

Supplementary Item (iv): Effect of interaction on $n(\mathbf{k})$

In the Bose-condensed phase, the $\mathbf{k} = \mathbf{0}$ component of the momentum distribution is reduced by unitary interactions, and the presence of a slowly-decaying k^{-4} tail at large k does not fully compensate this decrease. Therefore, the unitary-gas momentum distribution has a stronger weight in the intermediate-k region, as clearly visible in Fig. S4. In both the interacting and non-interacting case, $n(\mathbf{k})$ does not show strong finite-size effects at $k > 0$.

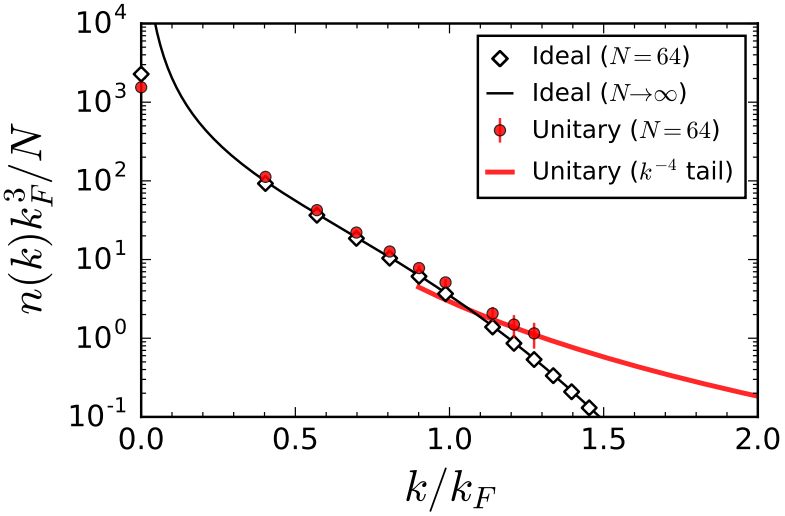

FIG. S4. Momentum distribution $n(\mathbf{k})$ in the Bose-condensed phase (point D in Fig. 3(a)) for the unitary Bose gas with $N = 64$ (same data as in Fig. 4(a)), compared to the curves for finite and infinite systems of ideal bosons at the same temperature.

Supplementary Item (v): Coexistence free energy

We consider N particles in a fixed volume V, in the presence of an l-particle nucleus of Efimov liquid. The coexistence free energy includes the liquid and gas contributions. For the liquid, we approximate $F_{\rm liq}(l) \simeq E_{\rm liq}(l)$, neglecting the entropic contribution, and we use the cluster energies from Ref. [10] for $l \leq 13$, in terms of the trimer energy $|E_T| \simeq 0.00214\,\hbar^2/(mR_0^2)$ [11]. For the gas contribution, we consider $N - l$ particles in a volume $V - V_{\rm liq}$ (where $V_{\rm liq} \simeq l \times (3.65R_0)^3$), and compute $F_{\rm gas}(N - l)$ up to the third virial coefficient[12]. At given values of N, V, and T, the coexistence free energy reads

$$F^N_{\rm coex}(l) \simeq E_{\rm liq}(l) + F_{\rm gas}(N - l). \tag{S1}$$

Computing $F^N_{\rm coex}(l)$ as a function of l allows us to check for the existence of a free-energy barrier $\beta\Delta F$, which does not disappear in the low-temperature regime. The third-order virial and cluster expansions differ in their range of validity, the cluster expansion being more accurate at low temperature (*cf.* Fig. 3(c)). We find that the above model is not quantitatively reliable at large R_0, for which the instability takes place at lower temperature. Its limit of validity is $R_0\rho^{1/3} \lesssim 0.04$, while for larger values of R_0 it does not correctly reproduce the coexistence line.

[1] D. M. Ceperley, Rev. Mod. Phys. **67**, 279 (1995).
[2] M. Boninsegni, N. V. Prokof'ev, and B. V. Svistunov, Phys. Rev. E **74**, 036701 (2006).
[3] T. Comparin and W. Krauth, "," In preparation.
[4] J. M. Diederix, T. C. F. van Heijst, and H. T. C. Stoof, Phys. Rev. A **84**, 033618 (2011).
[5] M. Rossi, L. Salasnich, F. Ancilotto, and F. Toigo, Phys. Rev. A **89**, 041602 (2014).
[6] A. G. Sykes, J. P. Corson, J. P. D'Incao, A. P. Koller, C. H. Greene, A. M. Rey, K. R. A. Hazzard, and J. L. Bohn, Phys. Rev. A **89**, 021601 (2014).
[7] D. H. Smith, E. Braaten, D. Kang, and L. Platter, Phys. Rev. Lett. **112**, 110402 (2014).
[8] E. L. Pollock and K. J. Runge, Phys. Rev. B **46**, 3535 (1992).
[9] L. P. Pitaevskii and S. Stringari, *Bose-Einstein Condensation* (Oxford University Press, Oxford, 2003).
[10] J. von Stecher, J. Phys. B **43**, 101002 (2010).
[11] E. Braaten and H.-W. Hammer, Phys. Rep. **428**, 259 (2006).
[12] Y. Castin and F. Werner, Can. J. Phys. **91**, 382 (2013), English version: arXiv:1212.5512.